Author's Accepted Manuscript

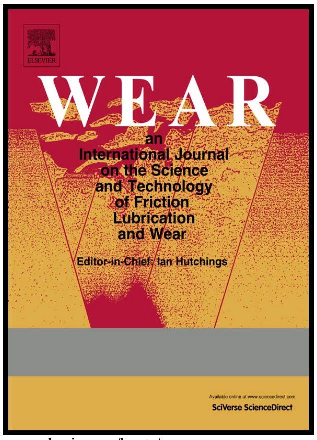

www.elsevier.com/locate/wear

Study of abrasive wear resistance of Fe-based nanostructured hardfacing

Agustín Gualco, Hernán G. Svoboda, Estela S. Surian

PII: S0043-1648(16)30049-7
DOI: http://dx.doi.org/10.1016/j.wear.2016.04.011
Reference: WEA101658

To appear in: *Wear*

Received date: 28 September 2015
Revised date: 7 April 2016
Accepted date: 11 April 2016

Cite this article as: Agustín Gualco, Hernán G. Svoboda and Estela S. Surian Study of abrasive wear resistance of Fe-based nanostructured hardfacing, *Wea* http://dx.doi.org/10.1016/j.wear.2016.04.011

Study of abrasive wear resistance of Fe-based nanostructured hardfacing

Agustín Gualco [1], Hernán G. Svoboda [2], Estela S. Surian [3]

[1] *Faculty of Engineering – National University of Lomas de Zamora, Camino de Cintura and Juan XXIII, (1832) Lomas de Zamora, Buenos Aires, Argentina and CONICET.* agustingualco@yahoo.com.ar
[2] *Faculty of Engineering – University of Buenos Aires, Las Heras 2214, (1427) City of Buenos Aires, Argentina and CONICET.* hsvobod@fi.uba.ar
[3] *Independent researcher.* esurianster@gmail.com

Abstract

In the last years several consumables which deposit hard nanostructured iron-based alloys with high resistance to abrasive wear have been developed. The microstructure of the weld metal usually shows variations with the welding procedure, particularly related to the heat input, number of layers and shielding gas type. The purpose of this work was to study the microstructural evolution and wear resistance of a nanostructured iron-based alloy deposited by FCAW process. Four samples with one and two layers were deposited under Ar-20%CO_2 shielding and without shielding gas, using a heat input of 3.5 kJ/mm. For each condition chemical composition was determined and microstructure was studied using both optical and electronic microscopy and X ray diffraction. Microhardness and abrasive wear resistance were measured. The microhardness of the deposit was found between 780 and 1020 HV_2, depending on the number of layers. There was a variation of the chemical composition between the first and the second layer. The wear test results were discussed in relation to chemical composition, microstructure and microhardness.

Key-words: *hardfacing; nanomaterials, number of layers, microstructure, abrasive wear.*

1. Introduction

Materials with nanometer microstructure size are called “Nanostructured Materials” (NM). The synthesis, characterization and processing of these NM are part of an emergent material market of rapid growth.

Recently and specifically in the welding area, various companies have developed iron based alloys with submicron grain structures. Their microstructures, with certain nano scale characteristics, show extraordinary properties which exceed those of microcrystalline normal grains materials [1-5].

In this sense, it was possible to develop Flux Cored Arc Welding (FCAW) tubular wires which generate nanostructured deposits with excellent wear resistance, reaching hardness values of 70 HRC, even with only one welding layer [1]. This high hardness is associated to an extremely small crystallite size of the matrix, ranging from 30 to 100 nm. These nano-microstructured materials present ultra-hard precipitates like niobium, boron and/or tungsten carbides and/or carboboride of chromium which improve abrasive resistance. They are applied on new or used parts or components, to provide specific properties such as resistance to abrasive and adhesive wear, corrosion, oxidation and their combinations [6, 7]. Recent statistics indicate that 50-60 % of equipment used in earthmoving or mining and mineral processing are worn by erosion and /or abrasion of high and low pressure, in humid or dry environment [6-8].

The abrasive resistance of FCAW deposits depends on several factors, but mainly on the microstructure, which defines their properties [6, 7]. Simultaneously, the heat input, the number of layers and the type of shielding gas strongly influence solidification and the dilution of the weld metal. Previous works [9-11] have shown that the increase of both heat input and number of layers produces changes in both the chemical composition and the microstructure of the deposits, and consequently in their properties. In nanostructured welding deposits, it has been observed that diluted deposit had different chemical composition which resulted in different precipitates and crystallite size of matrix as compared to originally designed microstructures[12]. On the other hand, it is well known that when shielding gas in not used in the welding process, the electric arc presents higher oxygen pressure, with a higher oxidation degree of several elements (Cr, Mn, Si, Nb, V, etc.), generating a lower concentration of these elements in the deposit and a probable lower wear resistance. As the consumable used in this work is recommended by the manufacturer for use with shielding gas or without it, this study was performed in both conditions. The objective of this work was to study the influence of number of layers on dilution, microstructure, microhardness and abrasive wear resistance in Fe-based nanostructured deposits obtained by semiautomatic welding process with shielding gas and without it.

2. Materials and methods

2.1. Weldments

The consumable used was a FCAW 1.6 mm diameter tubular wire. A Miggytrac System was applied for the movement of the torch. Table 1 shows the all-weld metal chemical composition specification of the manufacturer [13].

Table 1. All-weld metal chemical composition specification of the manufacturer (% wt/wt).

C	**Mn**	**Si**	**Cr**	**Nb**	**B**
<2	<2	<2	<18	<6	<6

Four coupons with 1 and 2 layers were welded with and without Ar-20CO_2 shielding gas. The welding parameters were chosen according to previous works [14]. The welding sequence was: 4 beads for the first layer and 3 for the second one, as shown in figure 1. The stick out was 18 mm under gas and 25 mm without it. The welding parameters are presented in table 2 as well as the sample identification. The inter-pass temperature was 150°C.

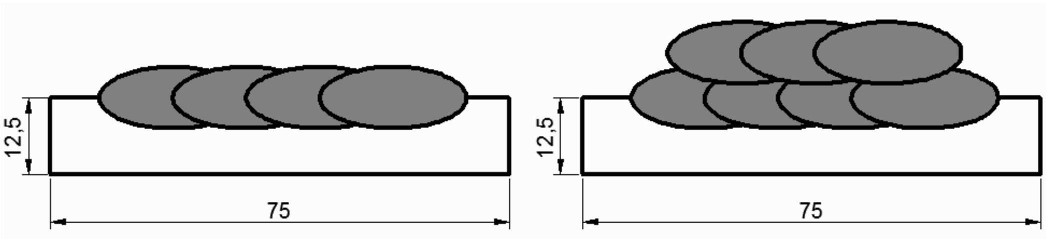

Figure 1. Welding sequence. Units in mm.

Table 2. Welding parameters.

Identification	**Layers**	**Shielding gas**	**Arc voltage (V)**	**Current intensity (A)**	**Welding speed (mm/s)**	**Heat input (kJ/mm)**
A1	1	Ar-20 CO_2	35	300	3	3.5
A2	2	Ar-20 CO_2	35	300	3	3.5
O1	1	-	35	300	3	3.5
O2	2	-	35	300	3	3.5

2.2. Chemical composition and microstructural characterization

The chemical composition was determined in the last bead by optical emission spectroscopy (OES). Boron was analyzed by plasma emission spectroscopy (PES). Local composition was analyzed by energy dispersive X-ray spectroscopy (EDS). The microstructures were observed on the cross section by light (LM) and scanning electron microscopy (SEM). The dilution was calculated from the geometry of the beads using an image analysis software [12].

On the hatched area of figure 2, X-ray diffraction (XRD) analysis was performed using a RIGAKU diffratometer, with radiation of Cu K-α, between 35° to 95º. The present phases were identified through phase analysis software, using data base and RIR (Reference Intensity Ratios) factors. The crystallite size was determined using the Scherrer equation [15].

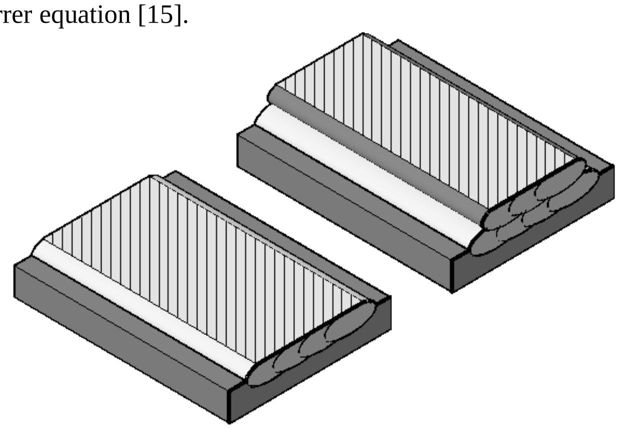

Figure 2. XRD measurement areas (12mm x 6mm).

2.3. Microhardness and abrasive wear resistance

On transverse sections Vickers microhardness (HV_2) determinations were carried out at 1 mm from the top of the layer, in a horizontal profile with a 2 mm distance between indentations.

The abrasive wear tests were performed according to ASTM G65-15 method A, using the dry sand/rubber wheel apparatus. The 25 mm wide and 75 mm in long abrasion test coupons were cut from single and double layer deposits. Roughness of specimens was 0.2 μm. The rotation velocity of the wheel was of 200 rpm, the flow rate of sand was 320 g/min and applied load was 130 N. The wear was evaluated by weight loss of the sample as average of three tests for each condition, after 4309 m.

3. Results and discussion

3.1. Visual inspection

In figure 3 the surface feature of the first layer is shown.

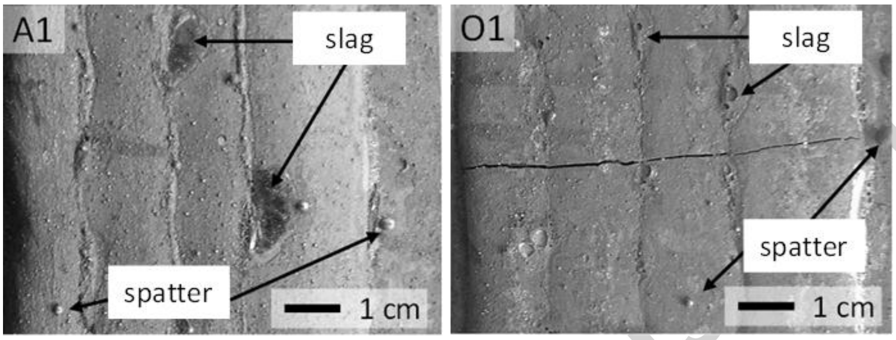

Figure 3. Appearance of the first layers.

In all samples, a low level of both spatter and slag was observed. Most of the beads contained cracks, produced by the stress relief, which is normal for this type of deposits.

3.2. Macroanalysis

Figure 4 shows the macrocuts of the different samples in which no macroscopic defects, porosities or inclusions could be seen except for the mentioned cracks.

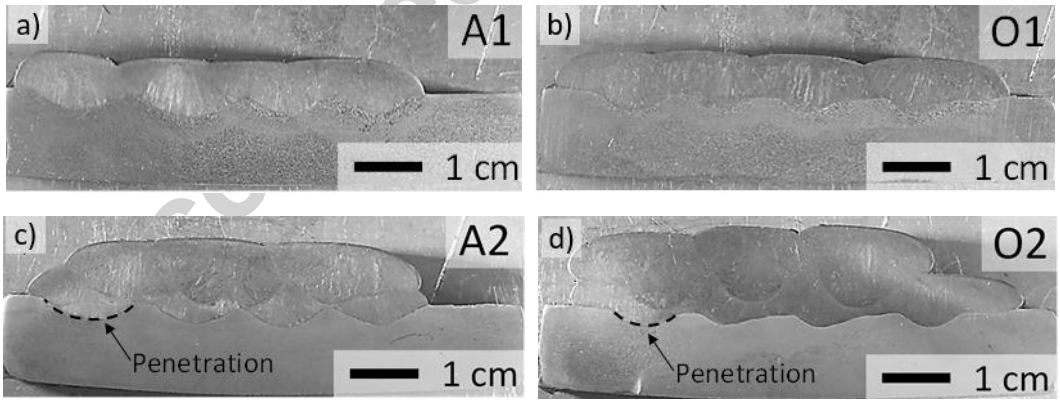

Figure 4. Transverse sections of welded coupons: one layer welded with a) Ar-20CO_2 and b) without shielding gas; two layer welded with c) Ar-20CO_2 and d) without shielding gas.

Figure 4 shows that the penetration was lower in samples welded without shielding gas. This could be associated with the change of transfer mode the spray to globular repelled. Dip and globular repelled transfer are commonly found with this type of consumable and very large levitated globular 'boots' may form at the wire tip [16].

The width of the beads deposited without shielding gas was higher than those samples welded under gas. This is attributed to the fact that an increased stick out produced a higher melting rate [16] and lower pressure of the arc and as a consequence higher width of bead. There were no important differences in the operational characteristics as a result of the use of shielding gas or not.

The dilutions were 35% and 28% for samples welded with and without shielding gas. It was observed that the samples welded without gas shielding had lower dilution. This could be related to the higher deposition of material and the lower penetration [6, 14].

3.3. Chemical composition

Table 3 presents the chemical composition results obtained from each sample.

Table 3. Chemical composition of each sample (% wt/wt).

	C	Mn	Si	Cr	Nb	B	Fe
A1	0.76	0.31	0.93	11.60	2.74	4.60	Bal.
O1	0.81	0.34	0.97	12.23	2.69	4.60	Bal.
A2	0.86	0.37	0.97	13.55	2.84	4.92	Bal.
O2	1.00	0.27	0.97	14.55	2.79	4.95	Bal.
Base metal	0.11	0.58	0.16	--	--	--	Bal.

For all the samples, the deposits presented a high level of alloying elements, inside the system Fe-(Nb.Cr)-(C.B).

Higher C, Cr, Nb and B contents were detected in the 2-layer samples, especially Cr in the samples welded without gas shielding. This is consistent with what was reported in previous papers [14]. This could be mainly related to the dilution (35% and 28%) and in minor proportion to the higher oxidation in samples welded without shielding gas. In this sense, the higher stick out produced an increase in the melting rate and as a consequence an extended oxidation time.

3.4. Microstructural characterization

In figure 5 the XRD patterns are shown.

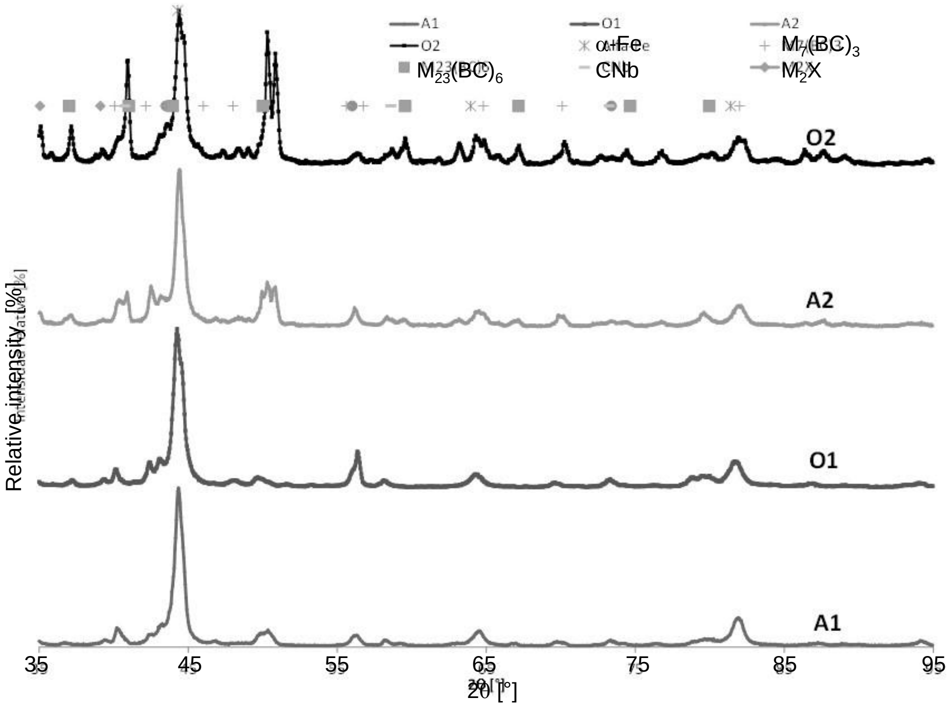

Figure 5. XRD patterns for the different conditions.

It could be seen that the microstructure was composed of α-Fe, with metallic carboborides [$(FeCr)_7(BC)_3$. $(FeCr)_{23}(BC)_6$] and niobium carbides (NbC). The crystallite size was between 80 and 120 nm: these variations could be related to the percentage of total precipitates, which could affect the distribution of the alloying elements [17, 18] and, as a consequence, the crystallite size.

In table 4 the percentage of the different phases in each sample is presented.

Table 4. Quantification of phases.

Sample	α-Fe [%]	$M_{23}(BC)_6$ [%]	$M_7(BC)_3$ [%]	NbC [%]
A1	55 ±3	18±1	26±1	1±0.5
O1	48±3	26±1	25±1	1±0.5
A2	41±3	33±2	24±1	2±0.5
O2	36±2	42±3	20±1	2±0.5

Table 4 shows that the two-layer samples presented higher quantity of $M_{23}(BC)_6$ precipitates, fact probably related to the lower dilution, that produces a deposit which is richer in alloying elements. This favors the mentioned precipitates formation [19-21]. Regarding the samples welded under gas shielding, they showed lower quantity of ultra hard $(FeCr)_{23}(CB)_6$ precipitates for 1 and 2 layers, associated with the lower Cr, B and C contents.

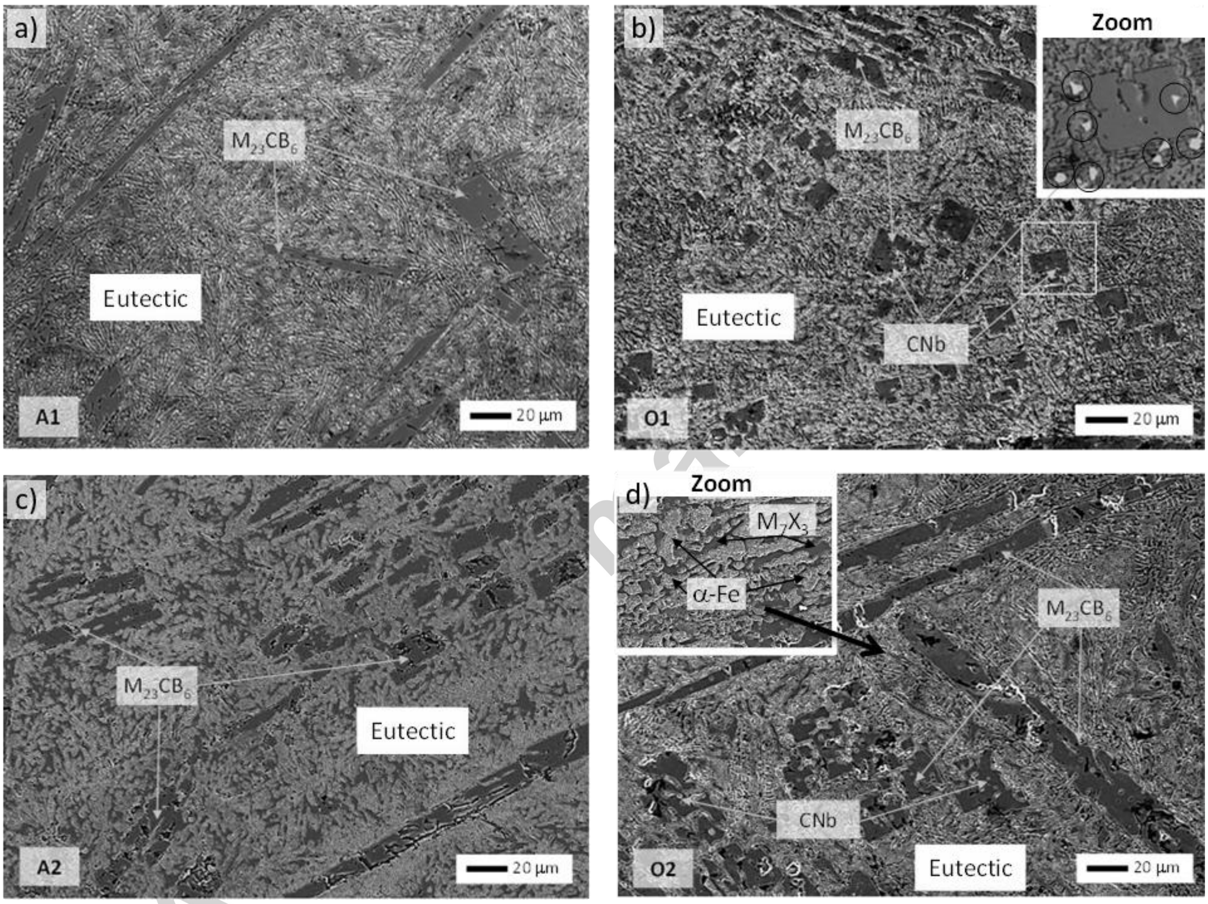

Figure 6. Microstructures on the cross section.

Figure 6 shows some Niobium carbides (NbC) of 2 to 4 µm size, elongate carboborides [$(Fe;Cr)_{23}(C;B)_6$] and the eutectic matrix formed by globular and flat plates of $(Fe;Cr)_7(C;B)_3$ in α-Fe. According to the literature [21-23] the first carbides to form during solidification are NbC; later, with the decrease of temperature, complex carboborides ($M_{23}X_6$) nucleated on them, as can be observed in figure 6; finally, from the remaining liquid the eutectic, α-Fe and M_7X_3 are formed.

It is also possible to see in figure 6 that the size and quantity of precipitates $M_{23}CB_6$ increased with the number of layers and in the samples welded without shielding gas. This is consistent with what was observed in the XRD spectra. This could be related to the dilution and lower cooling rate due to higher melting rate [16].

3.5 Microhardness

Microhardness, measured at 1 mm from the surface, results can be seen in figure 7.

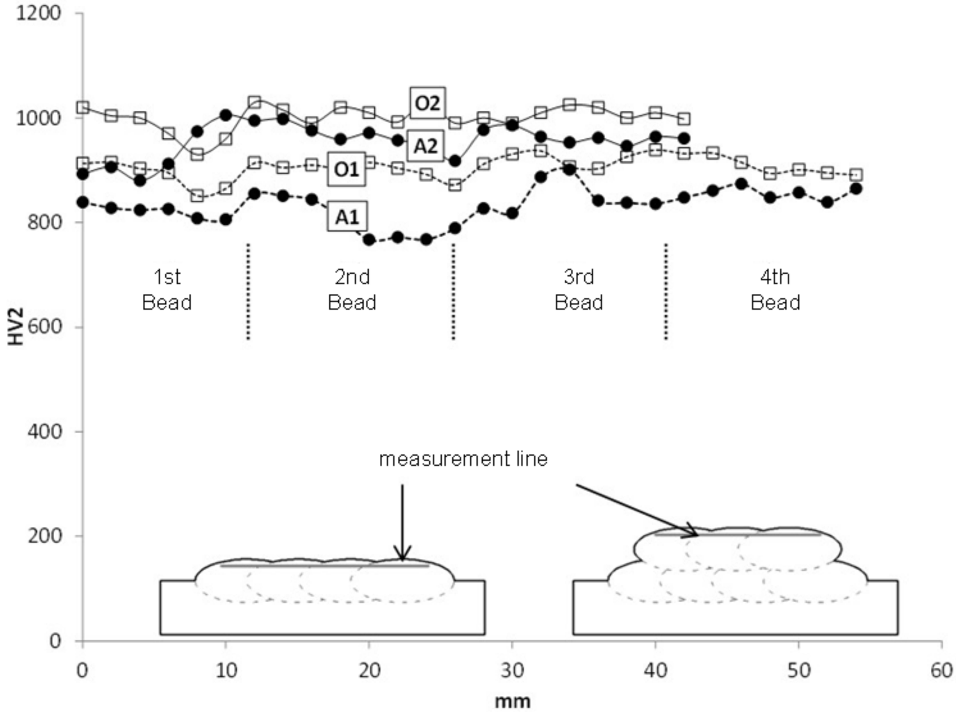

Figure 7. Microhardness results.

Microhardness values varied between 780 and 1020 HV, being consistent with the literature [20-21] for this type of materials. In the two-layer samples these values were higher than expected, fact associated with the higher alloying content which favor the formation of $M_{23}X_6$ of higher hardness, between 1400-1500 HV [3, 22]. Samples welded without gas protection showed higher hardness (comparing between the same number of layers samples) due to a higher fraction of ultra hard precipitates $M_{23}X_6$ present.

3.6 Abrasive Wear

The results of wear test are presented in figure 8. The weight loss of base metal was 2.2232 g.

For each condition the variation of mass loss was around 10 %. The two-layer samples showed a 30 to 40 % higher wear resistance, relative to those of only one layer, result associated to the higher degree of alloying elements. Samples welded without gas shielding had higher wear resistance, as expected taking into account the results presented in this paper.

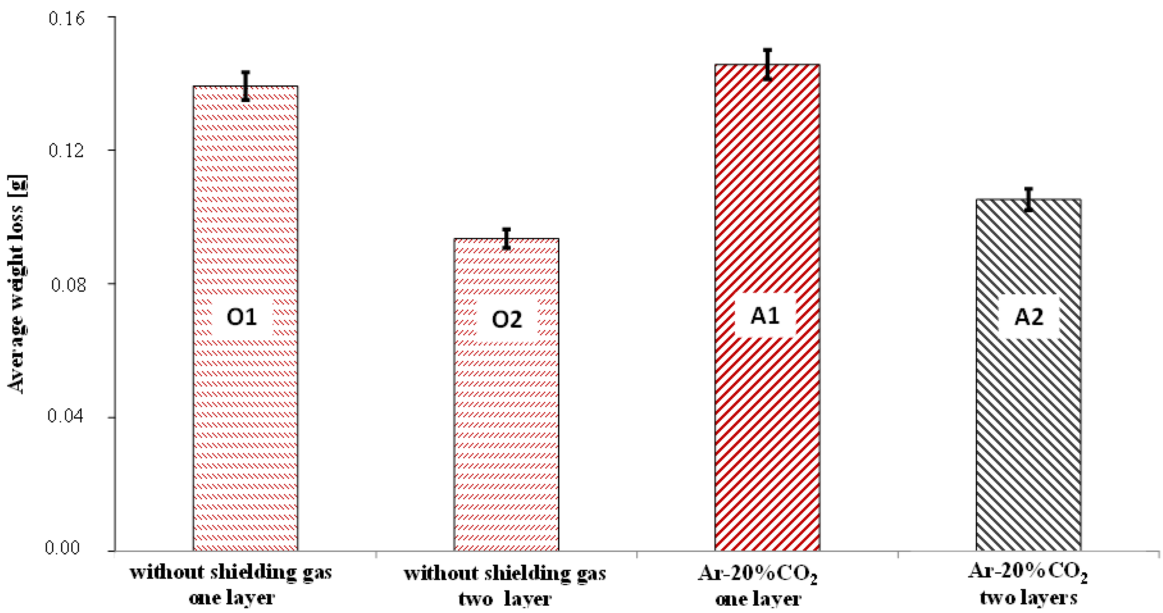

Figure 8. Weight loss values obtained in the wear test.

Figure 9 shows a SEM image of the worn surface. The analyzed area belongs to the centre of the worn surface. It is possible to see the abrasion grooves in the wear direction produced by the sand, in addition to the presence of precipitates confirmed by EDS. The width of the grooves was between 1 and 20 μm. The best abrasion resistance was obtained in the second layer of the complex carbides deposit, in which the elevated volume fraction of coarse $M_{23}X_6$ carboborides provided a barrier against indentation, grooving and cutting [24, 25]. This beneficial effect is probably reinforced by the NbC particles, which prevent the detachment of $M_{23}BC_6$ carbides due to their finely dispersed distribution in the matrix and their mechanical properties [26, 27].

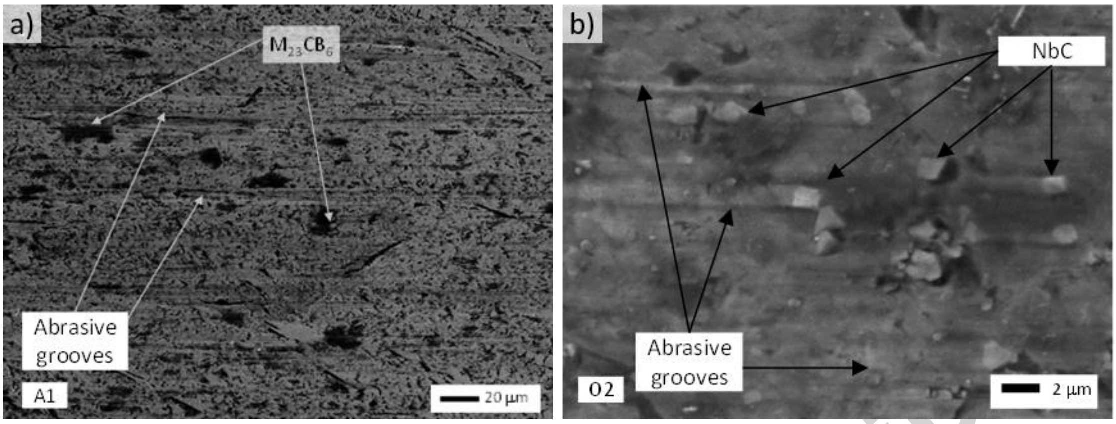

Figure 9. SEM image of the worn surface of samples a) A1 and b) O2.

Figure 10 presents the different sequences of abrasive wear.

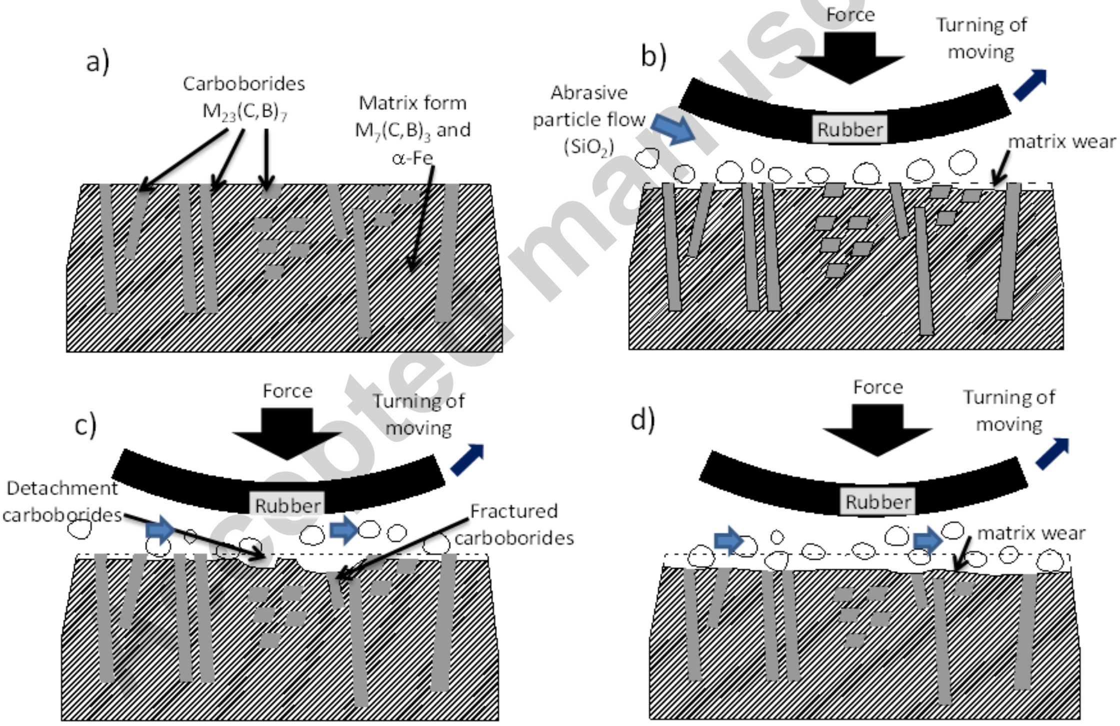

Figure 10. Sequences of abrasive wear a) Sample before abrasion; b) Preferential abrasion of matrix; c) Fracture of elongated carboborides by impact and scratching; d) Matrix abrasion again.

Based on reports by other authors [26], the wear abrasive process involves the following: the abrasive particles hit and impact the surface of the hardfacing, preferentially abrade the eutectic matrix, and gradually pick and dig up the matrix. This action gradually raises the carboborides $M_{23}(C,B)_6$, which reduces the strength against the external impact stress resulting in the crack or spalling of the elongated carboborides. This also promotes the wear of the matrix.

Figure 11 shows two longitudinal cuts of the samples wear tested.

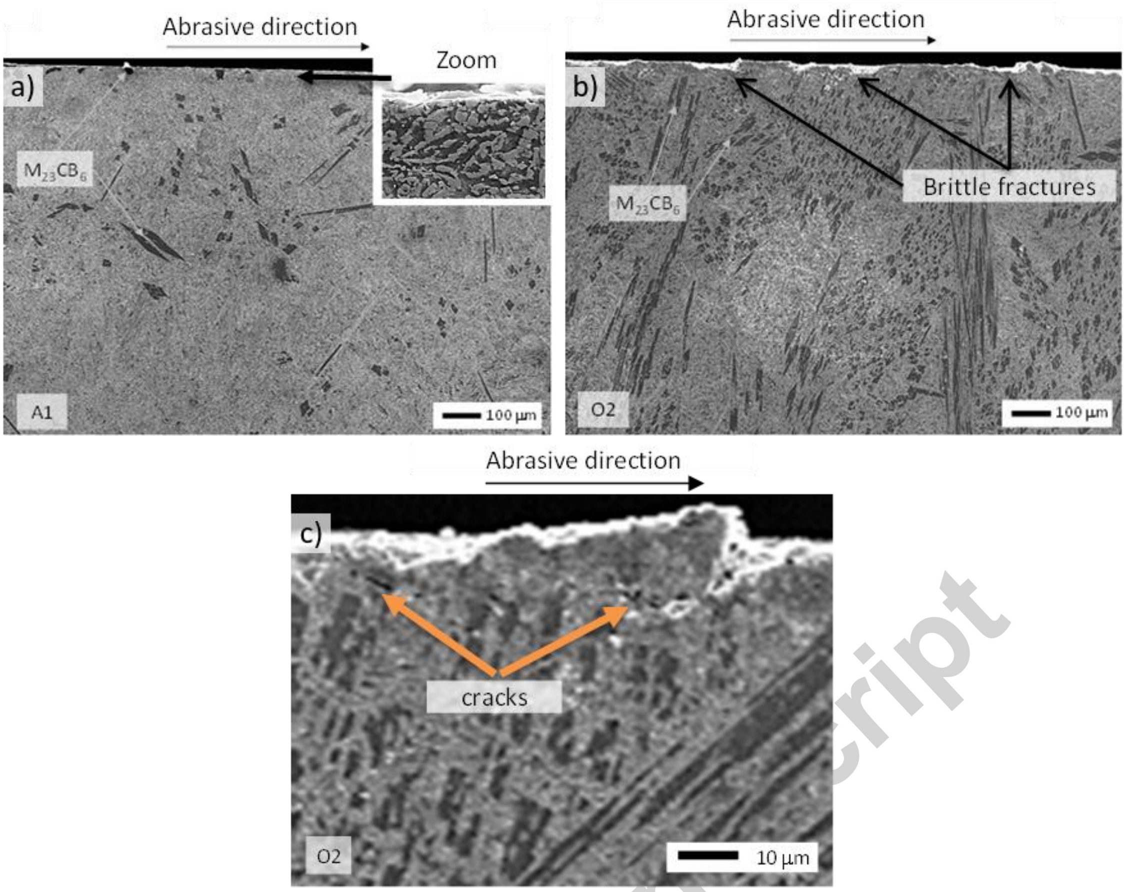

Figure 11. Longitudinal cuts of worn tested samples A1 and O2.

Figure 11 shows that the wear surface did not present plastic deformation on it. In complex carboborides, hardfacing alloys intense micro-cutting was observed when only one layer was applied, due to the absence of massive hard second phases in the microstructure (figure 11 a) [27-29]. In specimens with two layers brittle fracture of carboborides was observed, together with minor crack formation in $M_{23}X_6$ phase (figure 11 b and c) [30]. The predominant wear mechanism was microfracture. Sample O2, featuring two layers and welded without shielding gas, showed a higher quantity of ultra-hard precipitates, which is consistent with what was found in the XRD patterns. These elongated precipitates of around 100 µm, located perpendicular to the line of wear, are those which favor the wear resistance.

4. Conclusions

This work evaluated the effect of welding under gas shielding and without it and the number of layers on the characteristics of a Fe-based nanostructured deposit obtained from a FCAW tubular wire.

It was found that:

- All the samples showed low level of both spatter and slag. Most of them presented cracks during cooling.
- All the deposits had high level of alloying elements, inside the system Fe-(NCr)-(CB). The chemical composition varied with the degree of dilution, the two-layer samples welded without gas shielding showing the highest alloying content.
- For all the samples the microstructure was formed by a matrix α-Fe, metallic carboborides ($M_7(BC)_3$ and $M_{23}(BC)_6$) and niobium carbides (NbC). The crystallite size was between 80 to 120 nm. The two-layers samples presented higher $M_{23}(BC)_6$ precipitate content.
- Hardness values varied around 740 HV, for the one-layer sample welded under gas shielding, and 1020 HV for the two-layer sample welded without gas protection.
- Wear resistance was higher for the two layers samples and those welded without gas shielding.

According to the results obtained in this work and in the conditions here studied it seems not to be necessary to use this wire under gas shielding due to the fact that there were neither operational nor wear performance advantages when it is utilized. Of course, to use this wire in open arc is simpler and cheaper.

5. Acknowledgement

The authors wish to thank Eutectic-Conarco Argentina for the provision of the consumable used in this work, Air Liquide Argentina for the free supply of welding gases; Conarco-Esab Argentina for conducting chemical analyses; INTI-Electronic Microscopy Laboratory for the facilities of scanning electron microscopy and both APUEMFI (Association of Professors of Mechanics from the National University of Lomas de Zamora) and LomasC&T subsidy system for financial aid in this project.

6. References

[1] HEATH. G.. Nanotechnology and Welding – Actual and possible future applications. Proceedings of the CASTOLIN-EUTECTIC SEMINAR. Brussels: Belgium. 2006. p. 25-25.
[2] BRANAGAN D.J., Engineering structures to achieve targeted properties in Steel on a nanoscale level. Computer Coupling of Phase Diagrams and Thermochemistry, vol. 31, pp. 343-350, 2007.
[3] KIRCHGABNER M.; BADISH E.; FRANEK F. Behaviour of iron-based hardfacing alloys under abrasión and impact, Wear 265, pp. 772-779, 2008.
[4] KATSICH C.; BADISH E.; MANISH R.; HEATH G.R. Erosive wear of hardfaced Fe-Cr-C alloys at elevated temperature. Wear 267, pp. 1856-1864, 2009.
[5] YUKSEL N.; SAHIN S. Wear behavior-hardness-microstructure relation of Fe-Cr-C and Fe-Cr-C-B based hardfacing alloys, Materials and Design 58, pp. 491-498, 2014.
[6] MERRICK. S.; KOTECKI. D.; WU. J.. Materials and applications - Part 2. Welding Handbook. American Welding Society. 1998.
[7] LINNERT. G. E., Welding metallurgy carbon and alloy steels. 4 ed. AWS: Miami. Florida. 1994. 474 p.
[8] KLIMPEL. A; JANICKI. D. A study of worn wear plates of fan blades of steel mill fumes suction system. Proceedings of the 13th Scientific International Conference. Achievements in Mechanical and Materials Engineering" AMME'2005. Polonia: Gliwice. 2005. p. 307-310.
[9] EVANS. G. M. The effect of heat input on the microstructure and properties of C-Mn all-weld-metal deposits. Welding Journal. v.61. n.4. pp.125s-132s. 1982.
[10] GUALCO. A.; SVOBODA. H.G.; SURIAN. E.S.; de VEDIA. L. Effect of welding procedure on wear behavior of a modified martensitic tool steel hardfacing deposits. Materials & Design. v.31. n.9. pp. 4165-4173, 2010.
[11] FRANCIS. J. A.; Principles for open-arc weld deposition of high-chromium white iron surface layers. Adelaide Editor. 1999.
[12] WEISSMIILLER J. Alloy effects in nanostructures. Nanostructured Materials. v. 3. pp. 261-272. 1993.
[13] Datasheet: TeroMatec 395NOA. Eutectic Castolin-ESAB. USA. 2008.
[14] GUALCO. A.; SVOBODA. H.G.; SURIAN. E. S. Effect of Heat Input on the Fe-based Nanostructured Weld Overlay. Soldagen & inspecao vol 18, pp. 329-338. 2013.
[15]. CULLITY. B.D.; STOCK. S.R. Elements of x-ray diffraction. 3 ed. Prentice Hall. 2001. 520 p.
[16] NORRISH J., Advanced welding process-Technologies and process control. Woodhead Publishing Limited. 2006.
[17] GLEITER. H., Nanostructured materials: basic concepts and microstructure. Acta Materialia. v.48. n.1. pp. 1-29. 2000.
[18] INOE. A. Amorphous and nanocrystalline materials: Preparation, properties and applications. Springer. p.206. 2010.
[19] GUALCO. A.; RAMINI. M.; SVOBODA. H.G.; SURIAN. E.S; de VEDIA. L. Study of dilution on weld deposits for hardfacing. International Congress of Metallurgy and Materials SAM/CONAMET 2005. Mar del Plata. Argentina.
[20] GUALCO. A.; MARINI. C.; SVOBODA. H.G.; SURIAN. E.S. Effect of heat treatment on the Fe-based nanostructured weld overlay. IV Argentino Congress of Mecahnical Ingineering. Chaco. Argentina. 2014.
[21] BRANAGAN. D.J.; MARSHALL. M.C.; MEACHAN. B.E., High toughness high hardness iron based PTAW weld materials. Materials Science and Engineering A 428. pp. 116–123. 2006.
[22] ZHI. X.; XING. J.; FU. H., Effect of niobium on the as-cast microstructure of hypereutectic high chromium cast iron; Materials Letters 62. p 857–860. 2008.
[23] MAA. A; XINGA. J.; LIUA. S; Li. Y. Effect of chromium concentration on microstructure and properties of Fe–3.5B alloy; Materials Science and Engineering A. A 527. p. 6800–6808. 2010.

[24] KATO; K. Abrasive wear of metals. Tribology International. vol 30. 5. p. 333-338. 1997.
[25] ZUM GAH; K.H. Wear by hard particles; Tribology International. vol 31. 10. p. 587-596. 1998.
[26] FUJIMURA. H; NOTOMI. A. Development of hard overlay welding for high wear resistance; IIW DOC XII-1071-88, 1988.
[27] CHATTERJEE S., PAL T.K., Wear behavior of hardfacing deposits on cast iron; Wear 255, pp. 417–425. 2003.
[28] CHEN H.X., CHANG Z.C., Effect of niobium on wear resistance of 14% Cr with cast iron; Wear 166 pp. 197–201. 1993.
[29] BUCHELY M.F., GUTIERREZ J.C., LEON L.M., TORO A., The effect of microstructure on abrasive wear of hardfacing alloys, Wear 259, pp. 52-61. 2005.
[30] BUCHANAN V.E., MCCARTNEY D.G., SHIPWAY P.H., A comparison of the abrasive wear behaviour of iron-chromium based hardfaced coatings deposited by SMAW and electric arc spraying, Wear 264, pp. 542-549. 2008.

Highlight

- The crystallite size was between 80 to 120 nm
- Samples welded with two layers showed a higher quantity of ultra-hard precipitates
- Elongated carboborides provided a barrier against indentation, grooving and cutting
- NbC particles prevent the detachment of $M_{23}BC_6$ carbides
- Wear resistance was higher for the samples welded with two-layers